Open access • Journal Article • DOI:10.1116/1.569063

Influence of thermal radiation on the vapor pressure of condensed hydrogen (and isotopes) between 2 and 4.5 K — Source link

Cristoforo Benvenuti, R Calder, Giorgio Passardi

Published on: 01 Nov 1976 - Journal of Vacuum Science and Technology (American Vacuum Society)

Topics: Thermal desorption spectroscopy, Radiant energy, Thermal radiation, Desorption and Vapor pressure

EUROPEAN ORGANIZATION FOR NUCLEAR RESEARCH

CERN-ISR-VA/76-19
Closed distribution

THE INFLUENCE OF THERMAL RADIATION ON THE VAPOUR PRESSURE OF CONDENSED HYDROGEN (AND ISOTOPES) BETWEEN 2 AND 4.5 K

by

C. Benvenuti, R.S. Calder, G. Passardi

Abstract

Hydrogen molecules, physisorbed or condensed on cryosurfaces at liquid helium temperatures, can be desorbed by thermal radiation. The probability of the process depends on the nature of the cryosurface, the degree of H_2 coverage and the spectrum of the radiation. For a given spectrum the desorption rate is proportional to radiation intensity and, with a few exceptions, to the absorptivity of the cryosurface. The desorption efficiency of the absorbed 300 K radiant energy is approximately $7 \cdot 10^{-6}$ for most of the 20 bakeable cryosurfaces tested. A decrease of radiation temperature below 130 K causes a progressive reduction of the desorption efficiency which amounts to a factor of three at 80 K. This variation of efficiency can be fitted to a curve obtained by assuming that a threshold wavelength for desorption exists in the radiation spectrum at 45 μ. The energy carried by a photon of this threshold wavelength is about three times that required for the desorption of a condensed H_2 molecule. Precondensed sub-layers of heavier gas also introduce a decrease of the desorption efficiency - progressively in the order of HD; D_2; Ne; and A, N_2, Kr. For the last three gases the desorption efficiency is practically constant and independent of the substrate and the radiation temperature. Similar observations for the H_2 isotopes HD and D_2 are also reported. A physical model for the desorption process and its agreement with the results obtained here is discussed.

Geneva, May 1976

1. INTRODUCTION

Measurements of the saturated vapour pressure of solid hydrogen in different laboratories during the last decade[1),2)] have shown an unexpected deviation from the Clausius-Clapeyron equation

$$\log P_{sat} = A - B/T \qquad (1)$$

(P_{sat} is the H_2 saturated vapour pressure, T is the temperature of the condensing surface, and A and B are constants.) The deviation is towards a higher and temperature-independent H_2 pressure below $\sim$3 K.

In a first attempt to explain this departure, Chubb et al.[1)] have proposed that the anomalously high H_2 pressure or desorption rate, at low temperature, was induced by thermal radiation originating from warmer parts of the experimental apparatus. The results subsequently obtained at CERN[2),3)] and by Lee[4),5)] have confirmed this suggestion and have added the further indication that this effect of the thermal radiation on the H_2 desorption is strongly influenced by the nature of the substrate.

This unexpected behaviour of H_2 has severely limited the achievement of very low pressures by condensation cryopumping. Considerable effort has therefore been made at CERN both in the design of practical cryopumps, where the need is to lower the pressure by reducing the quantity of thermal radiation incident on the pumping surface, and in basic experimentation concerning the influence of the substrate on the desorption process. The preliminary results achieved in both these directions have been described in references 3), 6) and 7).

The present paper will review both the experimental results and the fundamental aspects of this radiation-induced desorption of H_2. The investigations have been extended to HD and D_2 in an attempt to obtain a better understanding of the physical mechanism of the desorption process.

2. EXPERIMENTAL

The results, which will be described in detail in section 3, have been obtained by means of several different cryostats, measuring instruments, and vacuum systems.

2.1 Cryostats

The first measurements were made using the model B cryopump[8] shown in figure 1. The experimental facilities provided by this cryostat were rather limited because neither the material of the condensing cryosurface (stainless steel) nor the quantity of thermal radiation incident on it could be changed easily. An improvement was obtained using the model C shown in figure 2. The main features and advantages are described in detail in reference 8); here we shall recall:

(i) the possibility of investigating the effects of the intensity and spectrum of the incident radiation by varying the transmission factor and the temperature of the cold screens, respectively,

(ii) the possibility of easily changing the cryosurface material and therefore of investigating its influence on the desorption of the adsorbed gas.

More recently, a third cryostat (model E cryopump shown in figure 3) with a silver-plated cryosurface, has proved to be useful and versatile for our measurements although originally designed as a practical cryopump[6].

2.2 Measurement accuracy

The experiments were directed at the measurement of the interdependence of the following basic quantities:

(i) gas pressure or density; (ii) temperature of the cryosurface; (iii) temperature of the blackened surfaces of the baffles which are used as the source of incident thermal radiation, (iv) degree of coverage (H_2, HD or D_2) on the cryosurface.

(i) Following the continuous development of ultrahigh vacuum techniques, a variety of total and partial pressure gauges have been used. The necessary continuity in the calibration of absolute pressure reading and linearity (at high pressures of H_2) has been obtained *in situ* using the H_2 saturated vapour isostere (see paragraph 3.1). The absolute position of this isostere on the pressure scale was determined by comparing it with a gauge previously calibrated by the dynamic expansion method. As a consequence of this procedure all the pressure measurements are affected by the same systematic error of approximately ±10% in addition to the random errors shown in the figures. During the early stage of the research an omegatron mass spectrometer permitting measurements down to the 10^{-13} torr range was used; more recently the investigations have been extended to the low 10^{-14} torr range by means of a quadrupole mass analyser

equipped with an electron multiplier. The random errors of the pressure measurements in all diagrams are not indicated unless exceeding ±5%. Thermomolecular corrections have been applied to all the data. This factor (i.e. $(T/T_o)^{\frac{1}{2}}$) corrects the gauge reading for the difference between the gauge operation temperature (i.e. T_o or ambient) and that of the condensate under consideration (i.e. T). In order to minimize the errors in the application of this correction due to a non-uniform temperature of the molecules, care was taken that the vacuum gauges could not "see" the cooled parts of the apparatus and that they were mounted on a measuring dome at a uniform and known (ambient) temperature. Finally, we have assumed that a standard Bayard-Alpert gauge has the same sensitivity for H_2 as for the H_2 isotopes. For each experiment the mass spectrometer was calibrated against the total pressure gauge.

(ii) The temperature of the cryosurface was regulated in the range 4.5 to 2.1 K by stabilizing the pressure on the liquid helium bath. It was stabilized and evaluated to ±0.01 K by measuring this helium pressure and using the helium vapour pressure tables.

(iii) The temperature of the blackened cold screens, used as a radiator, was measured by calibrated thermocouples distributed in such a way as to permit the control of the temperature uniformity in the enclosure surrounding the pumping surface. The estimated uncertainty in the temperature range 45 to 240 K is 1 K.

(iv) The degree of condensate coverage was estimated from the total quantity of the injected gas (evaluated from the pressure drop across an orifice of known conductance) and the geometrical area of the cryosurface. The effects of H_2 degassing from the walls of the vacuum system and of the pumping of the gauges have been discussed[8] and have been taken into account.

3. RESULTS

In a vacuum system pumped by a cryosurface the pressure is given by:

$$P = P_o + P^* \quad \text{with} \quad 0 < P^* < P_{sat} \quad \text{and} \quad P_o = Q/S \tag{2}$$

in which Q is the gas load, S is the pumping speed and P* represents the contribution to the pressure due to the desorption from the cryosurface (i.e. P* is the equilibrium pressure of the condensate).

This P* contribution is expected to increase with coverage and to reach a

final value (P_{sat}) depending only on the temperature of the cold surface and corresponding to the saturated vapour pressure of the gas being examined. However, in the case of hydrogen and its isotopes, both P* and P_{sat} were found to be influenced by the nature of the cryosurface and by the incident thermal radiation. In contrast, no variation of P* or P_{sat} was found with the following quantities which have been varied as indicated: (i) rate of condensate deposition (from 7×10^{13} to 7×10^{10} mol. $cm^{-2}s^{-1}$), (ii) temperature of the injected molecules (from 80 K to 300 K), (iii) ortho-parahydrogen concentration (from 1% to 75% of ortho). It was not possible to verify whether these measurements were influenced by the temperature of the cryosurface during the gas injection because of the hysteresis effects and transient phenomena which will be described in paragraph 3.1.

By measuring P_o and P, respectively before and after the injection of various quantities of gas, we have investigated the dependence of P* on temperature, condensate coverage and radiation load while considering the nature of the adsorbing surface as an additional parameter. The three parameters (i), (ii) and (iii) above have been chosen within the indicated ranges to suit the convenience of the various experiments, while the cryosurface temperature during the condensate deposition was fixed at 2.30 K unless stated differently.

The experimental data have been divided into four groups: adsorption isosteres, adsorption isotherms, effects of thermal radiation and cryosurface materials.

3.1 Adsorption isosteres

The adsorption isosteres for H_2, HD and D_2 are shown in figures 4, 5 and 6 respectively. The results in figures 4 and 5 and those indicated as (B) in figure 6 were obtained under identical conditions from the model B cryopump in which the cryosurface (stainless steel) received 9% of the ambient temperature radiation density since it was partially screened by imperfect copper baffles at a fixed temperature of about 80 K; the curve (E) of figure 6 was obtained by using the model E in which the silver-plated cryosurface was protected by blackened baffles at about 80 K transmitting less than 10^{-4} of the exterior 300 K radiation.

3.1.1 The form of the H_2, HD and D_2 adsorption isosteres strongly depends on the gas coverage.

(a) For coverages $> 0.9 \times 10^{16}$ mol. cm^{-2}, our isosteric data can be fitted at temperatures higher than about 3.0 K, 3.4 K and 4.1 K for H_2, HD and D_2 respectively, by a curve in the form of equation (1) with values of

A and B equal to 3.85 ± 0.1 and 41.6 ± 0.5 K for H_2, to 3.9 ± 0.2 and 52 ± 2 K for HD, to 4.1 ± 0.2 and 62 ± 2 K for D_2 for P expressed in torr and T in K. These give constant isosteric heats of 192 ± 2, 240 ± 8, 286 ± 8 cal. $mole^{-1}$ respectively. Furthermore, they all show the same qualitative deviation from linearity at lower temperatures which has been attributed to desorption produced by thermal radiation and which is discussed later. Figure 6, curve (E), clearly indicates that there are departures even when the adsorbate (in this case D_2, but the same is valid for H_2 and HD) is exposed to radiation coming only from surfaces at ∿80 K.

(b) At coverages below 0.3×10^{16} mol. cm^{-2} the pressures of the three gases are only very slightly dependent on the substrate temperature between 2.3 K and 4.2 K (see curves corresponding to 0.2×10^{16} mol. cm^{-2}).

(c) For intermediate coverages we have noticed two distinct and relatively complex temperature-dependent behaviours between 2.3 K and 4.2 K.

i) Between 0.3 and 0.6×10^{16} mol. cm^{-2} each temperature increase is accompanied by a transient pressure rise (not shown in figure 4) followed by a decrease to the indicated equilibrium values resulting in small net temperature dependence. These observations are strictly valid only for H_2. For D_2 this coverage range has not been investigated and the isostere of HD, corresponding to a coverage of 0.4×10^{16} mol. cm^{-2} (see figure 5) has shown a behaviour very similar to those of H_2 between 0.6 and 0.9 mol. cm^{-2}. This may be due to a mistake in estimating the HD quantity.

ii) Between 0.6 and 0.9×10^{16} mol. cm^{-2} the isosteres are at first (i.e. below a critical temperature of about 3.4 K for H_2, 3.8 K for HD and 4.4 K for D_2) temperature-dependent with a slope which increases with coverage and temperature and which finally approaches that corresponding to a fully saturated layer. Then (i.e. at the temperatures indicated) they present a discontinuity in which at constant temperature the pressure falls to a lower value (see vertical dotted lines in each of the three figures). Finally, above the critical temperatures they show transient pressure bumps as found at the lower coverages but the resulting equilibrium curve is now approximately parallel to the saturated

isostere. A subsequent temperature reduction results in return curves which are initially lower and then higher than the corresponding rising curves.

3.1.2 A few additional experiments have been made using the model B pump and adsorbing hydrogen on precondensed films of argon or neon (≈10 monolayers). These measurements, not included in the figures and reported here only semi-quantitatively, have provided the following information.

(i) For H_2 coverages higher than 0.9×10^{16} mol. cm^{-2} and 2×10^{16} mol. cm^{-2} on neon and argon substrates respectively, the temperature dependence of the H_2 vapour pressure above 3 K is the same as on bare stainless steel covered with more than 0.9×10^{16} mol. cm^{-2}. However, at 2.30 K we have observed a reduction from 2×10^{-11} torr (on bare stainless steel) down to 2×10^{-13} torr, i.e. a partial quenching of the radiation-induced "anomaly", and the deviation from linearity now appears clearly only below 2.6 K.

(ii) In contrast to the case of adsorption on stainless steel the isosteres on argon and neon for H_2 coverages lower than those indicated in (i) are always temperature-dependent. Furthermore, two discontinuities similar to those discussed above appear for H_2 on neon at about 3.4 K and 4.0 K for H_2 coverages of 0.5 and of 0.7×10^{16} mol. cm^{-2} respectively.

3.2 Adsorption isotherms

Various isotherms for H_2, HD and D_2 are presented in figures 7, 8, 9 and 10. Those in figures 7, 8 and 9 were obtained in the experimental situation described in 3.1 (i.e. model B cryopump with some radiation load from 300 K and stainless steel cryosurface). Those of figure 10 were obtained by adsorbing H_2 on MgF (upper curve) and on silver (lower curve) in the model C and E pumps respectively, where the cryosurfaces (at 2.30 K) were exposed only to radiation from 80 K (room temperature radiation transmission $< 10^{-4}$).

The most striking feature of these adsorption isotherms is that all the irregularities appear at surface coverages close to 0.3×10^{16} mol. cm^{-2} or multiples of this quantity (0.6 and 0.9×10^{16} mol. cm^{-2}). The only exceptions to this behaviour were observed on MgF_2 and argon substrates (see figures 10 and 9 respectively). In all other respects the isotherms obtained on bare substrates (figures 7, 8 and 10) are similar to each other and differ radically from those obtained on precondensed gas layers (figure 9). The two cases will

be described separately.

3.2.1 On bare substrates and below 0.3×10^{16} mol. cm^{-2} (quantity henceforth indicated as Q_o) all isotherms for a given hydrogen isotope overlap for temperatures between 2.3 and 4.2 K (see figures 7 and 8). The pressures in this coverage and temperature range are practically temperature-independent (see 3.1.1 (b)), and, in fact, are essentially determined by the desorption due to the infrared radiation reaching the cryosurface. Figure 10, furthermore, shows that in a low radiation situation the H_2 pressure at 2.30 K depends strongly on the nature of the cryosurface. At 2.30 K all these (bare substrate) isotherms present a peak at Q_o (at a slightly higher coverage for H_2 on MgF_2). The measured pressures below Q_o are stable when very low (i.e. for low radiation-induced desorption) but quickly decay above 10^{-10} torr. For example, in the case of H_2 adsorbed on stainless steel and completely exposed to room temperature radiation, the decay is so fast that no peak is seen.

With coverage above Q_o, the pressure either decreases or increases with coverage depending on the temperature. It reaches a constant value at $2\ Q_o$ for H_2 below 3 K and HD below 3.4 K (see figures 7 and 8, respectively). The corresponding isotherms for D_2 have not been obtained. Above these temperatures saturation is reached at coverages equal to $3\ Q_o$. The dotted lines in the coverage range between 0.6 and 0.9×10^{16} mol. cm^{-2} are representative of the hysteresis observed in the isosteres and described in section 3.1.1 (c).

When increasing the coverage above saturation and at $\simeq$2.3 K, the pressure decreases slowly with a slope which is increased both by the amount of the radiation-induced desorption (e.g. figure 10) and by the impurity level in the injected gases.

3.2.2 When H_2 is adsorbed on a precondensed layer of a less volatile gas, the following behaviour can be observed (see figure 9):

(i) The first low coverage part of the isotherm becomes temperature-dependent (e.g. H_2 on neon, see 3.1.2 (ii)) and the distinct peak at Q_o disappears leaving only a knee or a point of inflection.

(ii) Below about 3 K the saturation is reached at Q_o, while twice as much is necessary on metals.

(iii) At 4.2 K the saturation on neon is achieved at exactly the same concentration ($3\ Q_o$) as on metal surfaces, but now two distinct smooth steps appear at Q_o and $2\ Q_o$. Argon presents a more complex situation which is discussed in 4.1.2.

(iv) When H_2 is adsorbed at 2.30 K on HD or D_2, the progressive increase of the H_2 pressure with the condensing quantity up to Q_o is accompanied by a simultaneous decrease of the HD or D_2 pressure. Above Q_o the HD and D_2 pressures are constant and about ten times lower than the corresponding initial value. These results are not included in our figures.

3.3 The effect of thermal radiation on the H_2 vapour pressure

The radiation load was varied using one of two different techniques:

(i) screening the adsorbing surface from 300 K radiation with cold baffles (at ≈80 K) with different transmission efficiencies,

(ii) varying the temperature (between 50 K and 240 K) of these screening baffles (blackened, 0.9 emissivity) of which thermal radiation transmissivity ($\approx 10^{-5}$) was low enough to reduce the effects of the 300 K radiation to below our detection limit.

The first procedure, neglecting the 80 K contribution, maintains a constant 300 K spectral distribution of the incident photons. In the second case, both the intensity and the spectrum of the radiation are varied. The latter, because of the high ratios between the emissivities (≈13 in the less favourable case) and areas (≈3) of the irradiating and absorbing surfaces, was expected to approximate very closely to what would have been obtained in an ideal black body cavity. The results are presented in figure 11, where the H_2 pressure is plotted against the quantity of 300 K radiation absorbed (calculated from the He boil-off), and in figures 12 and 13 where the H_2 pressure is plotted against the fourth power of the radiating surface temperature. Note that all the pressure values in these three figures are for H_2 in saturated conditions at about 2 K.

From these results we can derive the following information:

3.3.1 For a constant spectral distribution of the radiation (here corresponding to 300 K), the H_2 pressure varies proportionally with the quantity of the absorbed radiation (see figure 11).

3.3.2 The measurements obtained for H_2 condensed on MgF_2 and on nickel (curves A in figure 12) and on silver (figure 13) show a deviation from linearity when varying the temperature of the screen which indicates that the desorption efficiency (torr ℓ per incident watt) of the radiation decreases progressively with decreasing temperature of the irradiating surface. More particularly, these

non linear results can be fitted by the relation (see full line in figures 12 and 13):

$$P_{sat} = \overline{P} + \alpha \cdot \sigma^{-1} \int_{0}^{\lambda_0} I(\lambda,T)\, d\lambda \qquad (3)$$

in which $\overline{P}$ is the expected normal saturated vapour pressure (i.e. extrapolated from high pressure data using the Clausius-Clapeyron equation) which has been rendered negligible in all the following measurements by working at sufficiently low temperature; $I(\lambda,T)$ is the Planck expression in which T is the temperature of the radiating surface and λ is the radiation wavelength; σ is the Stefan-Boltzmann constant; $\lambda_o = 45 \pm 5$ microns; α is a constant equal to $(1.7 \pm 0.1) \times 10^{-19}$ torr K^{-4} for MgF_2, $(1.7 \pm 0.1) \times 10^{-20}$ torr K^{-4} for nickel, and $(2.2 \pm 0.1) \times 10^{-20}$ torr K^{-4} for silver. Physical arguments explaining the meaning of this equation are given in section 4.

Previous measurements (see reference 2)) obtained on a stainless steel condensing surface, showed a different behaviour of P_{sat} which was reported to be linearly dependent on the fourth power of the baffle temperature in the range 90 K to 300 K. Further experiments (the results are not shown) have actually indicated that this apparent difference was produced by the residual level of 300 K radiation and that H_2 does in fact behave on stainless steel the same as on the three materials considered here.

Figure 13 shows that radiation power from 77 K gives for H_2 on a silver surface a pressure of 3.3×10^{-13} torr, a value which is higher than that reported in reference 3). We believe that this discordance lies within the errors of our earlier measurements.

3.3.3 In another experiment, we have investigated the behaviour of an unsaturated layer of H_2 by adsorbing on MgF_2 the quantity corresponding to the peak of the isotherm at 2.3 K (see figure 10). For baffle temperatures below about 130 K, P* followed equation (3), being, however, about twice the corresponding saturation pressure. A further temperature increase was accompanied by a pressure decay, the rate of which increased progressively with the temperature towards the corresponding saturation values (see also 3.2.1).

3.3.4 By precondensing a thin film of nitrogen on MgF_2, on nickel and on silver (see respectively the curves (B) of figure 12, squares and circles, and the lowest curve of figure 13) we have observed the following effects:

(i) A large reduction of the desorption efficiency of the radiation, resulting in lower saturation pressures which are then all very similar to each other (within ±20%) in spite of the large pressure differences (a factor of ten) observed without the nitrogen layer (compare, for example, the curves A and B of figure 12).

(ii) A linear dependence on the fourth power of the irradiating surface temperature. In fact all the resulting measurements can now be fitted by the simple relation

$$P_{sat} = \overline{P} + \alpha T^4 \qquad (4)$$

in which $\overline{P}$ has the same meaning as in equation (3) and α is now equal, for the three experimental situations, to $(6.5 \pm 1.5) \times 10^{-22}$ torr K^{-4}.

3.3.5 When a rare gas layer has been precondensed on the same silver substrate P_{sat} follows the equation (4) with $\alpha = (1.5 \pm 0.1) \times 10^{-21}$ torr K^{-4} for neon (i.e. about twice that for nitrogen) and with $\alpha = (6.5 \pm 1) \times 10^{-22}$ torr K^{-4} for argon and krypton (i.e. the same as that for nitrogen within our measuring precision, see figure 13).

3.3.6 If the precondensed gas layer is D_2, the H_2 pressure follows the equation (3) with a value of α about 10 times lower than that obtained without precondensed D_2 on the same substrate (MgF_2). In other words, the precondensed layer, while reducing the H_2 desorption rate, does not produce the linear dependence given by equation (4) and obtained with the other gases.

3.3.7 All the $P\text{-}T^4$ plots have been obtained while increasing the radiation load. The corresponding return curves coincide with the rising curves above about 90 K but below this temperature they show a deviation (only evident on bare surfaces) resulting in lower saturation pressures (e.g. H_2 on silver, figure 13).

3.3.8 The extension of the investigation to deuterium condensed on bare MgF_2, Ni and Ag has provided pressures systematically lower than the corresponding values for H_2 (approximately a factor of 50) and a linear dependence on T^4. Unfortunately, these results were found to be scarcely reproducible and therefore they cannot be quoted with complete confidence. Precondensed layers of heavy gases (argon and nitrogen) led to still lower deuterium saturation pressures which were very near to our measuring limits (10^{-15} torr range for deuterium).

The results described in paragraphs 3.3.3, 5, 6, 7 and 8 are not shown in our figures with the exception of the cases of H_2 on neon and silver (see figure

13) and the return curve for H_2 on silver (open circles in figure 13).

3.4 Variation of the cryosurface

Besides the precondensed layers of gas and the surfaces already mentioned, many other materials have been tested for use as a cryosurface. These investigations were motivated by an attempt to find a better substrate for practical applications (i.e. that yielding the lowest H_2 saturation pressure for a given radiation load, and possibly the lowest liquid He consumption). Altogether about 20 different substrates have been tested. They were selected following various criteria, with the only common requirement of compatibility with ultra-high vacuum and bakeable to 150°C or higher. The results are shown in figure 14. All the measurements are from single samples, except Ag(1), for which seven samples have been tested either on the C or E cryopumps. In this case all the results lie within the indicated uncertainty and the samples were all made by electro-depositing silver on stainless steel (thickness of the layer about 20 μ). The same technique was used for Ni and Au. A few materials (pyrex, inconel, stainless steel, beryllium, copper) were used in bulk to make the liquid He container which provides the cryosurface. Finally, all the others were obtained by vacuum deposition, either by evaporation (Pb, Al, MgF_2, In and Si, Ge, AgCl, CsI - the last four, see below, not shown in the figure), or by sputtering (Ag(2)); in these cases the thickness of the deposited layers was about 1 μ.

All the materials shown in figure 14 were tested in the same situation, i.e. in a cavity at 300 K. The radiation density will be very close to that of a black cavity when the materials under test have a low absorptivity in the infrared range, but it will deviate from this situation for increasing absorptivities. In order to compare the data the measured pressures (corresponding to saturation, i.e. about $10Q_0$ of adsorbed H_2) have been plotted against the amount of absorbed radiation (in mW per cm^2 of cryosurface as deduced from the He boil-off). Figure 14 shows that practically all the materials (only exceptions are stainless steel and inconel) yield an H_2 saturation pressure roughly proportional to the amount of absorbed power. The corresponding desorption efficiency, defined as the ratio of the desorption power (sublimation energy × desorption rate) to the total power absorbed, is therefore almost substrate-independent (5×10^{-6} to 1×10^{-5}).

A few other materials were tested but are not reported in this figure because they are partially transparent in the infrared and, since only 1 μ thick, the measured radiation absorption was primarily in the underlying substrate. These

materials were Si, Ge and AgCl on stainless steel and CsI on both stainless steel and silver. All the observed results were similar (a slight increase of radiation absorption accompanied by a proportional increase of the H_2 saturation pressure) with the exception of CsI on stainless steel where a 10% increase in radiation absorption was accompanied by a reduction in the H_2 saturation pressure of a factor of about 2.5.

4. DISCUSSION

4.1 Dependence of the equilibrium pressures on the coverage and temperature of various substrates

4.1.1 From the experimental data reported in sections 3.1 and 3.2 we have concluded that the quantity Q_o, with its multiples, plays a central role in the adsorption phenomenology of all the hydrogen isotopic species. Not only is the adsorption isotherm of H_2 on neon at 4.17 K (figure 9) a clear example of stepwise multilayer adsorption isotherm[9], but other arguments seem to prove that Q_o corresponds to the monolayer capacity:

(i) On the one hand, Q_o must represent at least this quantity, because the isotherms of H_2 on HD and D_2 at 2.30 K and on neon at 2.92 K show saturation at Q_o (see figure 9) and because this same amount of H_2 quenches the pressures of underlying HD and D_2, at 2.30 K, to a level which is practically independent of a further H_2 adsorption (see 3.2.2, iv).

(ii) On the other hand, the complete absence, below Q_o, of any observable pressure variation in the adsorption isosteres on bare substrates (e.g. figures 4, 5, 6) indicates a very low temperature-dependent equilibrium pressure, i.e. high adsorption energy, which is probably available only for the first admonolayer. The observed pressure is then attributed to radiation-induced desorption.

4.1.2 All the data presented in figures 4, 5 and 6 can be easily correlated on the basis of this assumption to those of figures 7, 8, 9 and 10. The following picture then emerges:

(i) two monolayer quantities of H_2 below ≈3.4 K and of HD below ≈3.8 K are required for saturation on bare surfaces. This can be seen in figures 4 and 5 where the isosteres at 0.6×10^{16} mol. cm^{-2} show discontinuity at these temperatures. Above these temperatures, up to 4.2 K, three monolayer quantities are necessary. Consequently, one

finds that any adsorption isostere obtained for coverages between two and three monolayers and low radiation load overlaps the saturated vapour pressure isostere below these temperatures. Then, above these temperatures, the amount of adsorbed gas is not sufficient to provide saturation, and the isosteres show the discontinuities described in 3.1.1 (c); more generally, a discontinuity in the adsorption isostere at a given temperature corresponds to the appearance of an additional step in all isotherms above this temperature because a further monolayer is required for saturation.

(ii) On precondensed gas layers (figure 9) H_2 shows saturation already at one monolayer below ≈3 K and at three monolayers at 4.17 K. On the other hand, two discontinuities have been observed at ≈3.4 K and ≈4 K in the adsorption isosteres of H_2 on neon (see 3.1.2, ii). Therefore between these temperatures two monolayers would be necessary to achieve saturation.

Only two of the reported isotherms deviate from this general quantitative behaviour: those of H_2 on MgF_2 at 2.30 K (figure 10) and on argon at 4.17 K (figure 9). In both cases the H_2 quantities involved are approximately twice the normal values. In the first case the cause is probably a higher surface area presented by the MgF_2 substrate (obtained by evaporation), while in the second case the reason is almost certainly the diffusion of H_2 in the argon film, because the saturation quantity increases with the argon film thickness and because the equilibrium times are much longer than on other substrates.

Less attention has been devoted to the above problems and to their fundamental implications than to the radiation effect, which had more direct influence on the design of the cryopumps. However, we believe that the discontinuities in the adsorption isosteres represent a rearrangement of the monolayer initially providing saturation from a bulk-like structure to a structure more influenced by the underlying substrate.

4.2 The radiation effect

Different physical models have been proposed by Lee[4),5)] and by the present authors[2)] to describe the mechanism of the infrared radiation-induced desorption.

4.2.1 Lee suggested that some radiant energy is absorbed in the solid hydrogen layer as lattice vibrations. Due to the barrier for the transport of heat between dissimilar solids, a temperature difference is generated across the condensed gas-metal interface according to:

$$T_1 = (T_2^4 + c^2Q/5\cdot10^9\Gamma)^{\frac{1}{4}} \qquad (5)$$

where T_1 and T_2 are the temperatures of the first and second medium, c is the velocity of sound in the first, i.e. the gas adlayer, Q is the heat flow and Γ is a function of the densities and sound velocities in the two media. By inserting T_1, given by equation (5), in (1) and by a suitable choice of the ratio of Q to Γ, Lee was able to construct isosteres very similar to those obtained experimentally for fully saturated adsorption.

However, this interpretation does not fully account for our experimental results; in particular the following points would seem to be at variance with this model:

(i) If the anomalous pressure is produced by absorption of radiation in the H_2 layer, a regular increase of the desorption rate with thickness of the adsorbed layer would be expected. Instead, a maximum desorption at the completion of the first monolayer followed by a continuous decrease with increasing gas coverage is observed, see 3.2.1 and figures 7, 8 and 10.

(ii) The form of the relationship between pressure and quantity of absorbed radiation, obtained from the insertion of (5) in equation (1), does not agree with that shown in figure 11, where the measurements were obtained without changing the spectral distribution of the incident radiation.

(iii) The deviation from linearity described by equation (3) together with its disappearance with precondensed gas layers (see 3.3.4 and 5) cannot be described by this model.

4.2.2 Rather, we have suggested[2] that the incident photons traverse the condensed gas layer before making their first interaction at the surface of the condensing substrate. There, phonons are generated which propagate back through the H_2 or HD or D_2 films and, before being thermalised, cause molecules to be desorbed.

(i) The linear dependence of the H_2 pressure on the amount of infrared radiation absorbed by the various cryosurfaces, shown by figure 14 (with a few exceptions which will be discussed later) supports the hypothesis that the desorption process originates at the level of the substrate.

(ii) The absorbed radiation produces phonons which, to cause gas release, must be transmitted to the admolecules and provide them with enough energy to break the adsorption bond.

The Debye temperatures of solid H_2 and its isotopes, taken here as an indication of the maximum transmissible phonon frequency, are lower than those of the materials used as substrates. Therefore, when a few monolayers of these gases are adsorbed, that fraction of the phonons whose frequency exceeds the Debye frequency of the adsorbed gas cannot be transmitted back through the gas film. From figures 7 and 8 the isotherms at 2.30 K suggest that the filtering action is already well established at the completion of two monolayers. However, near or below the monolayer coverage, on the contrary, this effect is not present and it is reasonable to expect a more pronounced radiation effect - hence the presence of the peak in the 2.30 K isotherms at the completion of the first monolayer.

A concomitant cause of the peak could be found in the excitation of surface phonons of frequency much higher than that of the volume phonons and whose appearance is predictable[10] when the admolecules have a very small mass.

Finally, the observed decrease of the pressure with the increase of the condensed H_2 thickness and/or impurity level (see 3.2.1) may be imputed to the higher scattering probability of the phonons in their propagation to the H_2 surface. Some sort of similar argument might also be invoked to describe the smaller effect of the radiation in the case of metal alloy substrates (stainless steel and inconel) when compared with pure metals, see figure 14.

(iii) Precondensed layers of a less volatile gas are expected to introduce an even greater reduction of the radiation effect[2]. In fact, the Debye temperatures of all the solidified gases examined here are lower than that of H_2, and therefore the cut-off of the phonon spectrum is displaced towards lower energies. Both the disappearance of the desorption maximum (see figure 8) and the reduction of the H_2 saturation pressure, observed when a thin film of condensed gas is interposed, seem to support our model. A good qualitative agreement is provided by isotherms at 2.30 K of H_2 on stainless steel and on precondensed HD, D_2 and Ne (see figure 9), which show a decreasing desorption rate with the Debye temperature Θ_D of the underlying gases

(respectively: H_2, 110 K; HD, 100 K; D_2, 95 K; Ne, 60 K)[11].

However, the extension of this investigation to films of argon, nitrogen and krypton precondensed on silver and exposed to different radiation loads (see 3.3.5) did not confirm this relationship. These gases all give similar pressures which are approximately a factor of two lower than those corresponding to neon in spite of the different Θ_D (respectively: A, 90 K; N_2, 70 K; Kr, 60 K)[11]. The reason for this uniform behaviour is not clear. A tentative suggestion is that these relatively heavy gas molecules have a very poor mobility when condensed at 4 K and hence cannot develop a well defined crystal structure. In this case the significance of the Debye temperature and its role as defining the upper cut-off limit for the transmission of phonons becomes questionable. Such a non-crystalline layer could well exhibit a virtually zero phonon transmission - hence practically all effects of both the underlying substrate and the condensed substrate could be lost. The small residual and substrate-independent desorption would then be attributed to a direct interaction of the radiation with the condensed hydrogen.

When using the same precondensed layer of a light gas on various substrates, different H_2 pressures may be expected even under similar radiation conditions. This behaviour has been observed when precondensing D_2 before H_2 on stainless steel and on MgF_2. The ratio of the H_2 pressures in the absence to that in the presence of a D_2 film was practically the same for the two substrates, i.e. about ten, cf. the isotherms at 2.30 K in figure 7 for H_2 on stainless steel with that for H_2 on D_2 in figure 9, see 3.3.6. However, a precondensed layer of a heavy gas (e.g. N_2) has provided an opposite result. In fact, in the presence of N_2 the pressures of H_2 on MgF_2 and nickel are practically equal, while in its absence they differ by a factor of ten (see figure 12). This behaviour is again in agreement with that which could be expected from the deposition of a heavy gas forming a non-crystalline or 'snowy' intermediate layer.

(iv) The sublimation energy for a molecule of condensed H_2 is 1.33×10^{-21} joules, or 100 K in terms of temperature, i.e. lower than the Debye energy for phonons in solid H_2 (110 K). This simple consideration suggests that the desorption of an H_2 molecule may be produced by a single phonon, i.e. it may be a first order process initiated by

single photons. The reduction of the radiating temperature depletes the radiation spectrum in these high frequency photons, and the desorption efficiency of the radiating power might be expected to decrease. The corresponding experimental results shown in figures 12 and 13 (upper curves) and described by equation (3), confirm this suggestion. Equation (3) has been obtained on the basis of the observed linear dependence of the H_2 pressure, both with T^4 at high radiating temperature and with the incident power at constant radiation spectrum, and of the additional hypothesis that above a given wavelength (λo) the photons are unable to desorb H_2. The meaning of λo is therefore that of a phenomenological threshold; quantitatively, the corresponding photon carries about three times the energy necessary for desorbing a molecule of condensed H_2.

A precondensed layer of gas with a Debye temperature lower than 100 K prevents the transmission to the H_2 film of the phonons able to produce, individually, molecular desorption. The desorption efficiency of the radiating power should therefore decrease greatly, in agreement with the results which indicate, for example, a factor 30 decrease for N_2 precondensed on silver. Furthermore, it should become irrelevant whether or not the incident photons can produce energetic phonons, since in any case these now cannot reach the H_2 film; hence the disappearance of the threshold indicated by the linear dependence of the H_2 pressure on T^4 (lower curves of figures 12 and 13).

When D_2 is used as an intermediate layer the H_2 behaviour is still described by equation (3), although the cut-off frequency of D_2 is only 95 K, i.e. lower than the 100 K required for single phonon desorption. However, the difference is small and probably within the uncertainty of the D_2 data.

(v) The materials which are transparent, or semi-transparent, in the infrared deserve special comments. In fact, they might behave as precondensed gases when their Debye temperature is below about 110 K. Among the transparent materials tested, only CsI belongs to this category, and it has actually provided a pressure reduction on a stainless steel substrate. On the other hand, no reduction was noticed when a CsI layer was deposited on a silver substrate, and in general this material did not provide reproducible results.

Always, according to our model, a transparent material with a Debye temperature higher than about 110 K should present a rather passive behaviour, i.e. no H_2 pressure reduction, and this has been observed with Si, Ge, AgCl. This generalisation could not be tested by injecting and precondensing a gas since no suitable gaseous material was found with Θ_D above 110 K.

5. CONCLUSIONS

The experimental results clearly confirm that the anomalously high and temperature-independent vapour pressure of solid hydrogen (and its isotopes) is a result of desorption stimulated by incident thermal radiation. Details of the behaviour indicate that the mechanism of desorption is one in which the incident radiation first produces phonons when interacting with the substrate. A fraction of these phonons travels back into the hydrogen and produces this desorption.

The desorption rate, or pressure, depends linearly on the quantity of absorbed radiation (i.e. incident radiation times substrate emissivity) at constant incident spectrum. It is partially quenched either by a reduction of the temperature of the incident thermal radiation or by a precondensed sub-layer of a heavier gas. The first effect is interpreted as showing an energy threshold for desorption by the incident photons. The second effect is described in the model by assuming that the interposed layer of gas with a Debye temperature lower than that of H_2 acts as a low pass filter and reduces (HD, D_2) or prevents (N_2, A, Kr) the return of the energetic phonons which are responsible for the H_2 desorption. In the latter case the small residual desorption rate, now independent of both substrate and precondensed gas, is ascribed to that minor fraction of the incident radiation which interacts directly with the condensed hydrogen.

The variation of the H_2 pressure with the quantity of adsorbed and/or condensed gas also presents many interesting features, especially in the range up to and including a few monolayers. Not surprisingly the observed pressure generally increases with this coverage but at the lowest temperatures and on bare substrates, where the radiation-induced desorption is the dominant effect, the pressure passes through a clear maximum at Q_o (estimated at 3×10^{15} mol. cm^{-2}). This peak in the adsorption isotherm may be caused by an effect similar to the pressure reduction observed when precondensing another gas below the H_2. In the present case the lower layer(s) of hydrogen may impede the propagation to the surface of high frequency phonons originating both in the substrate and in

the gas-substrate interface where additional high frequency surface modes are made possible by H_2 adsorption.

At surface coverages below one monolayer the H_2 condensate seems to be strongly adsorbed to the substrate and the observed pressure, which is generated by and varies with the incident radiation, is practically independent of the substrate temperature. For larger coverage the H_2 isosteric curves exhibit discontinuities (structural rearrangements?) and hysteresis when heating and cooling the cryosurface. These discontinuities and the temperatures at which they occur are related to the inflexion in the isotherms and the corresponding number of monolayers required to achieve saturation. The generalised picture is that in passing from the lowest temperatures of 2.3 K up to 4.2 K, one or two and finally three monolayers are required to reach saturation.

6. ACKNOWLEDGEMENTS

The authors are indebted to E. Fischer for continuous encouragement and useful comments, and to R. Mundwiller for his conscientious and valuable technical assistance.

REFERENCES

1) J.N. Chubb, L. Gowland, J. Pollard, Brit. J. Appl. Phys., Ser. 2, 1, 361 (1968).

2) C. Benvenuti, R.S. Calder, Phys. Lett. A 35, 291 (1971).

3) " " , Le Vide (Suppl.) 157, 29 (1972).

4) T.J. Lee, Proc. 3rd Int. Cryogenic Conf., Berlin, 388 (1970).

5) " , Nat. Phys. Sci., 231, no. 26, 193 (1971).

6) C. Benvenuti, J. Vac. Sci. Technol., Vol. 11, 3, 591 (1974).

7) " , D. Blechschmidt, G. Passardi, Le Vide (Suppl.) 169, 117 (1974).

8) " , CERN Report no. 72-3 (1972).

9) J.H. Singleton, G.D. Halsey, J. Phys. Chem., 58, 1011 (1954).

10) G. Armand, P. Masri, L. Dobrzysnsky, J. Vac. Sci. Technol., 9, 2, 705 (1971).

11) E.S.R. Gopal, Specific Heats at Low Temperatures, p. 33. Heywood, London (1966).

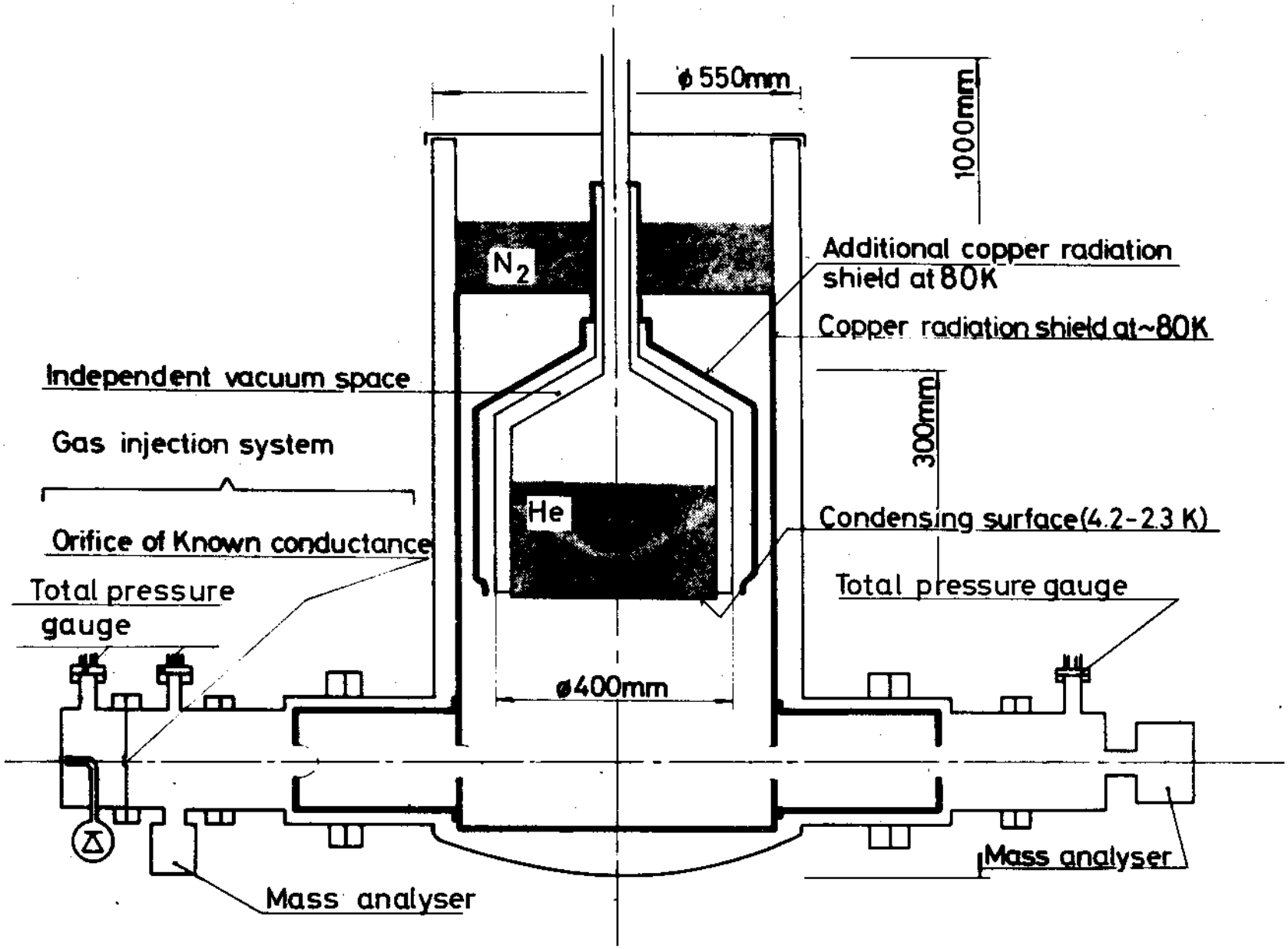

Fig. 1. Model B cryopump and measuring equipment

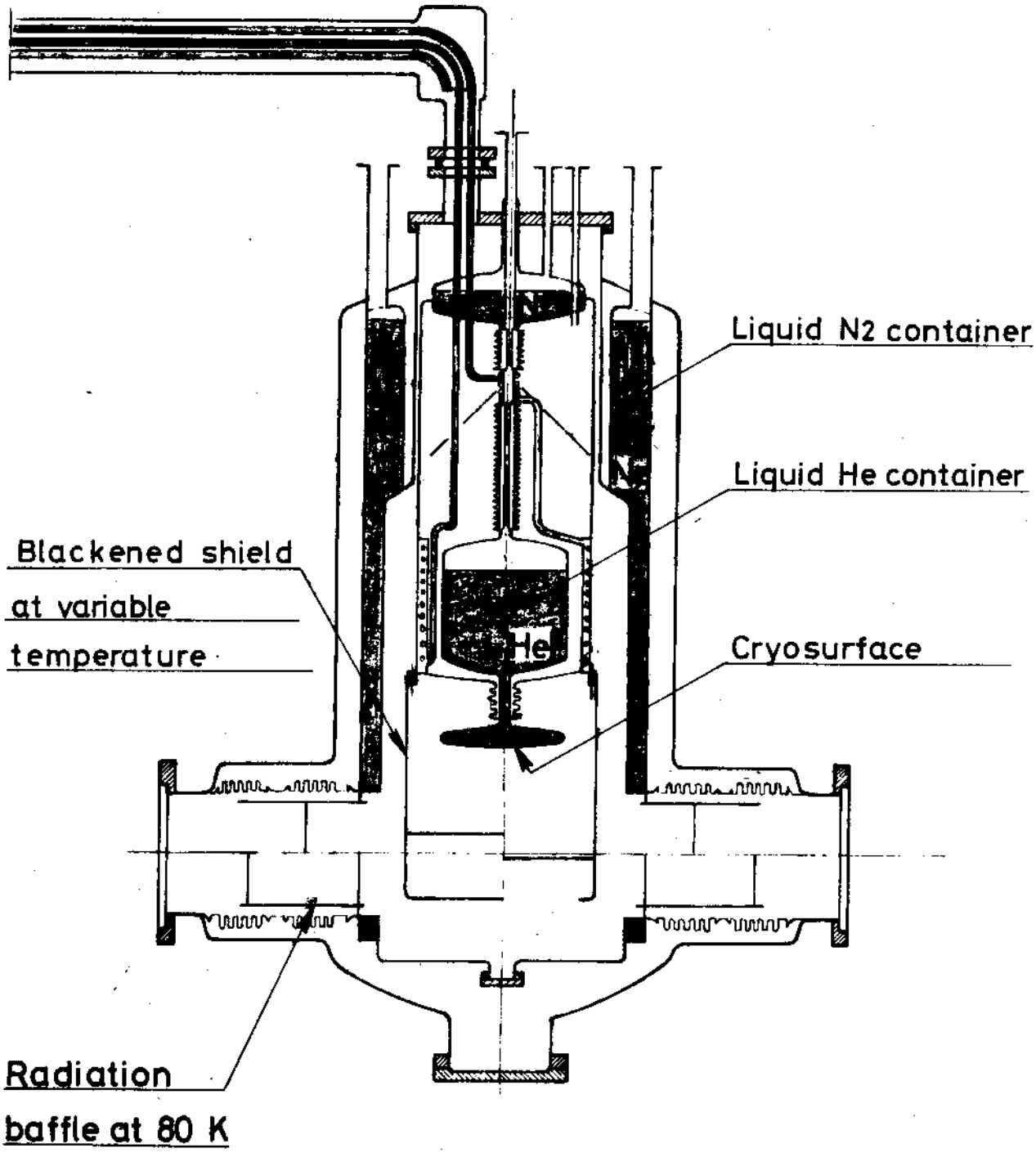

Fig. 2. Cryostat for the optimisation of the cryopump parameters (model C)

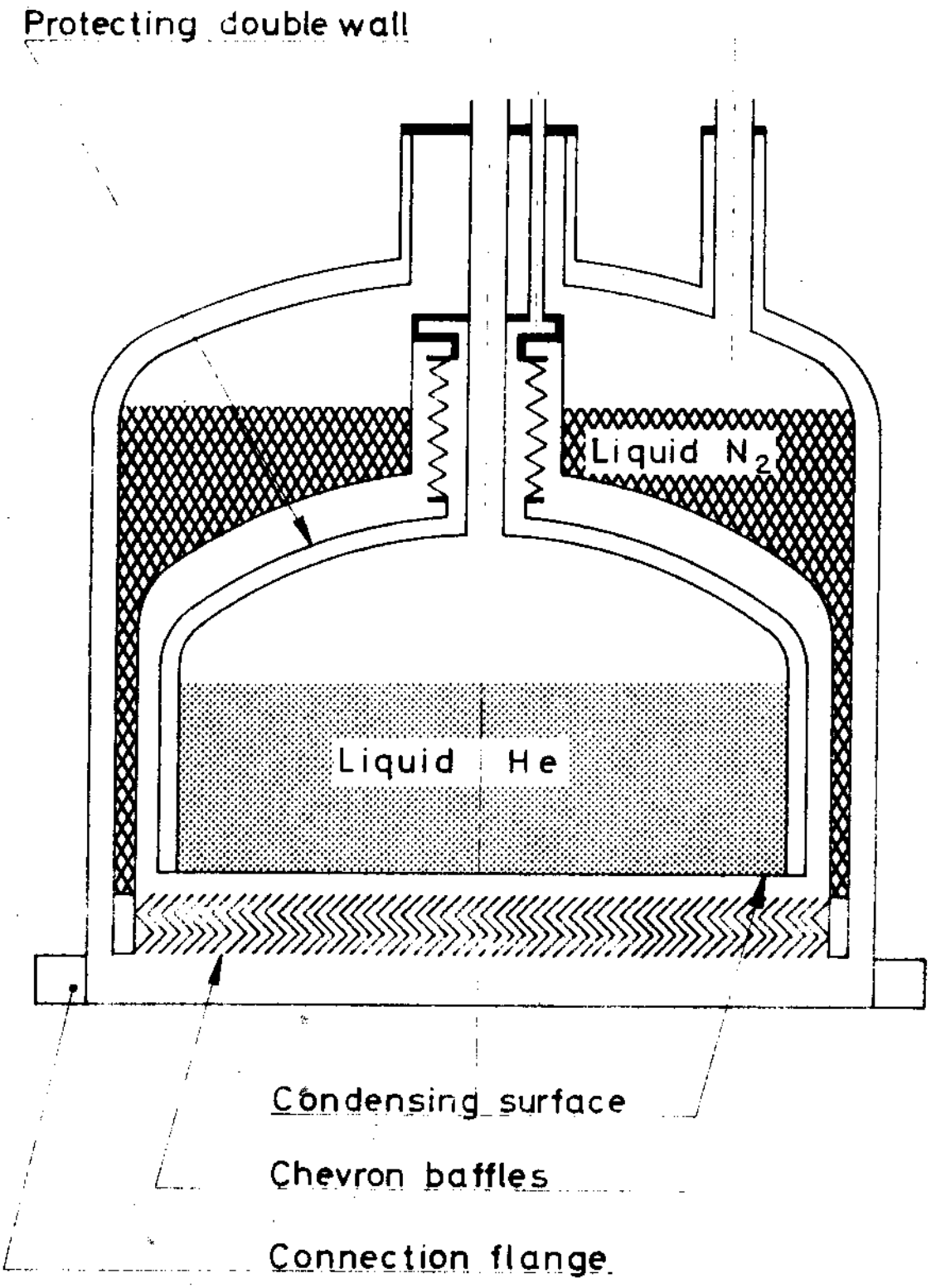

Fig. 3. Model E cryopump - optimised design used in UHV systems

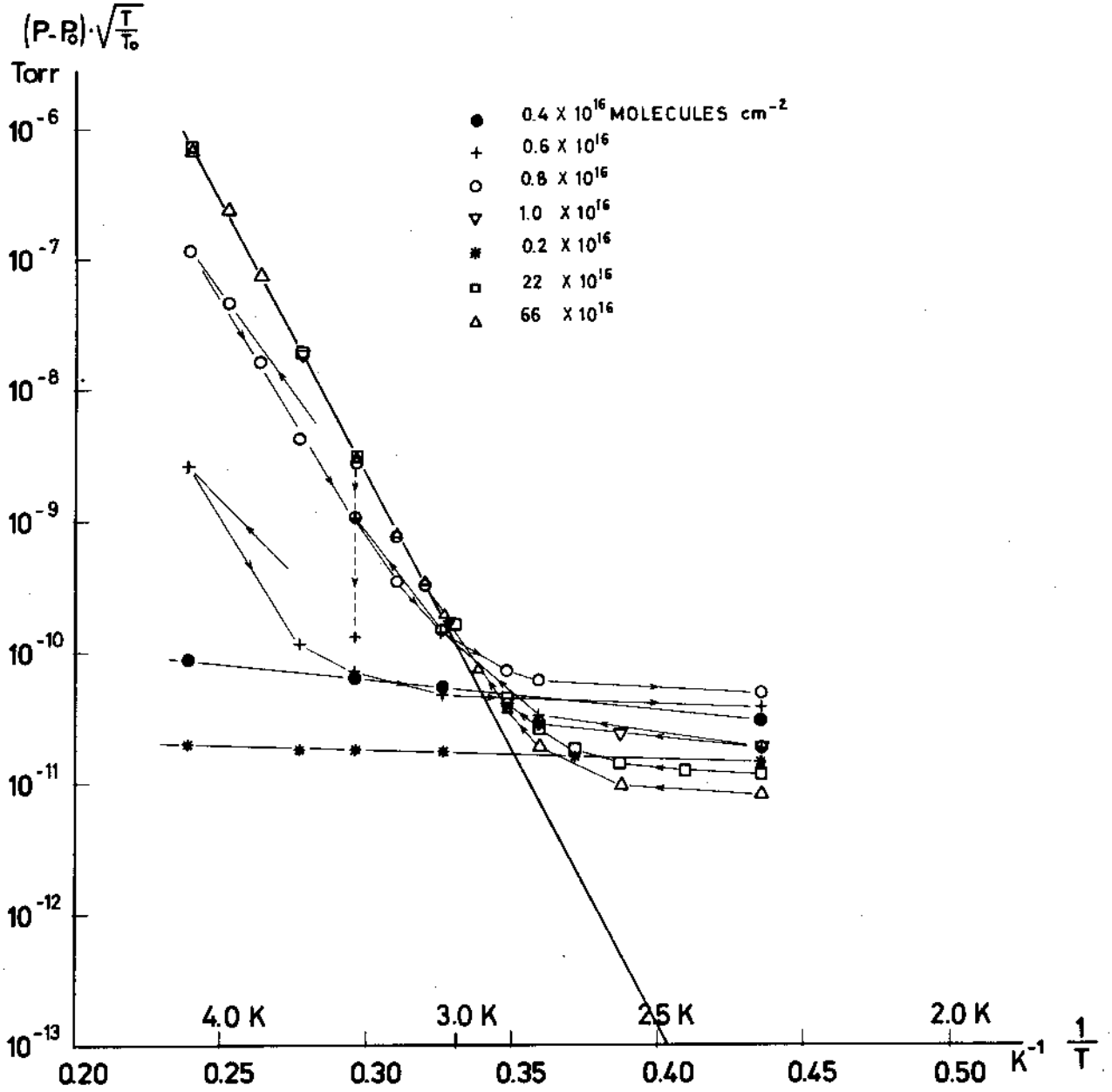

Fig. 4. Adsorption isosteres for H_2 on stainless steel cryosurface partially exposed to radiation from 300 K.

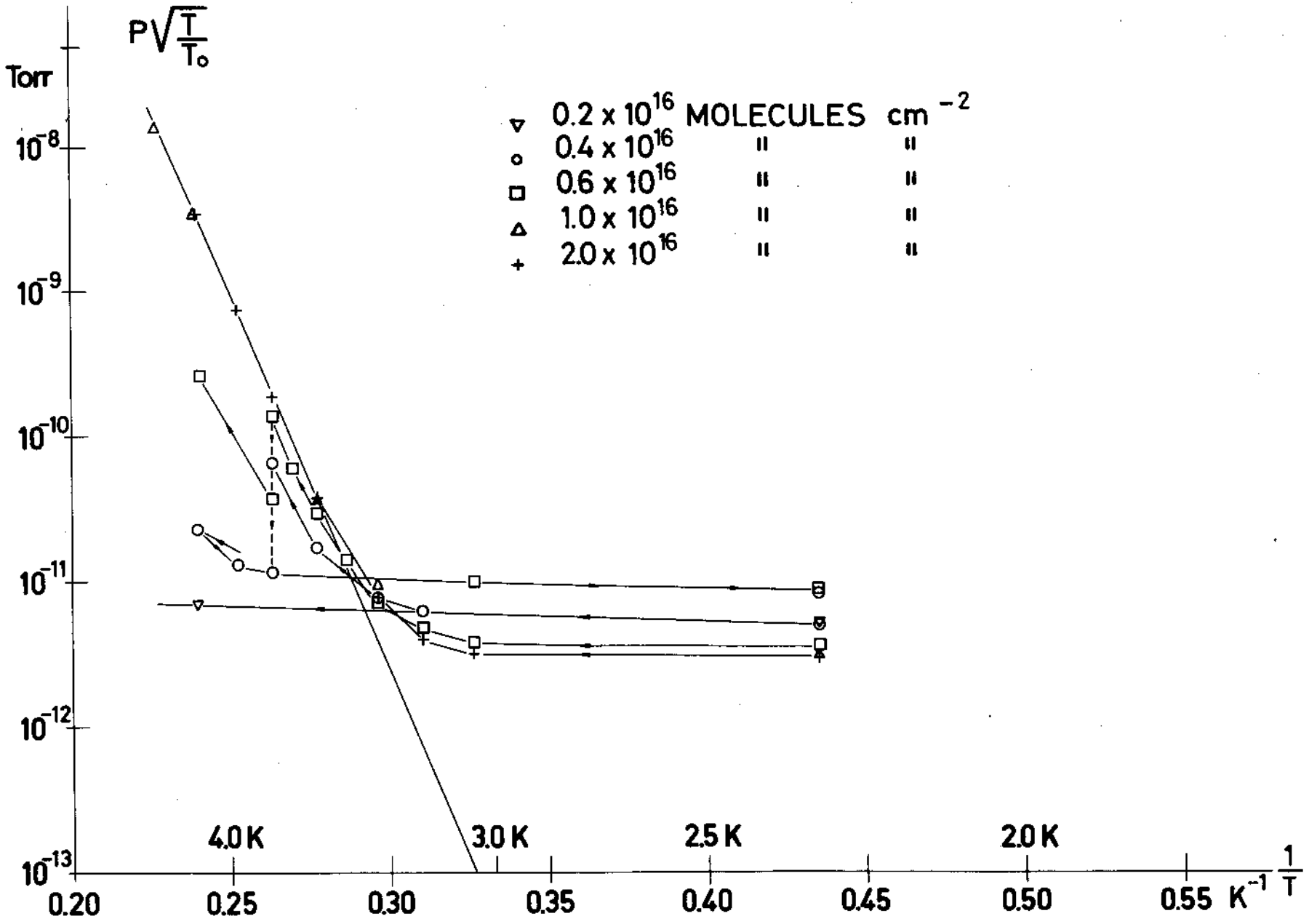

Fig. 5. Adsorption isosteres for HD on stainless steel cryosurface partially exposed to radiation from 300 K. The HD contribution from P_o is zero.

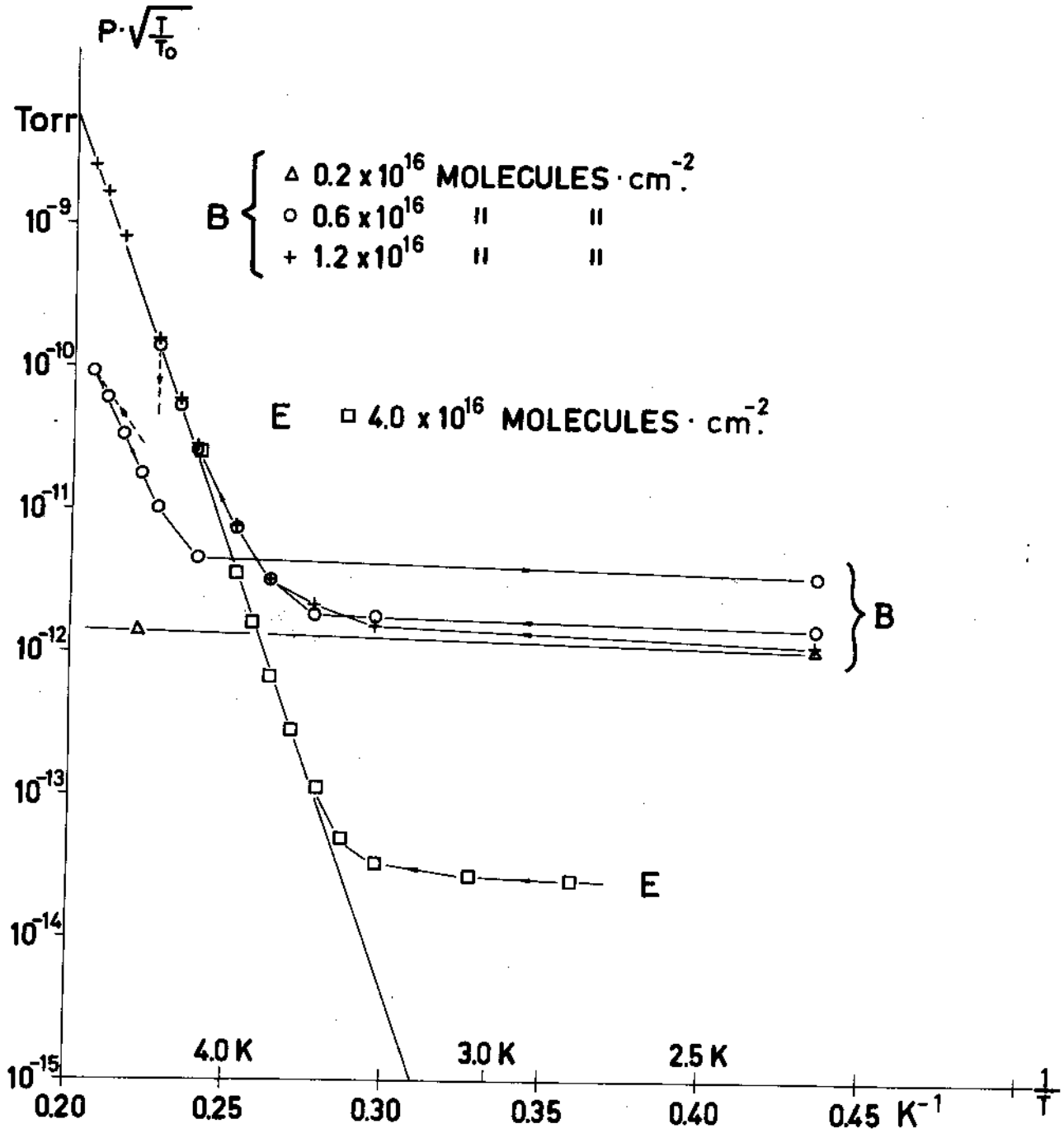

Fig. 6. Adsorption isosteres for D_2. Curves B, stainless steel cryosurface partially exposed to radiation from 300 K; curve E, silver plated cryosurface exposed to radiation from about 80 K only. The D_2 contribution from P_o is zero.

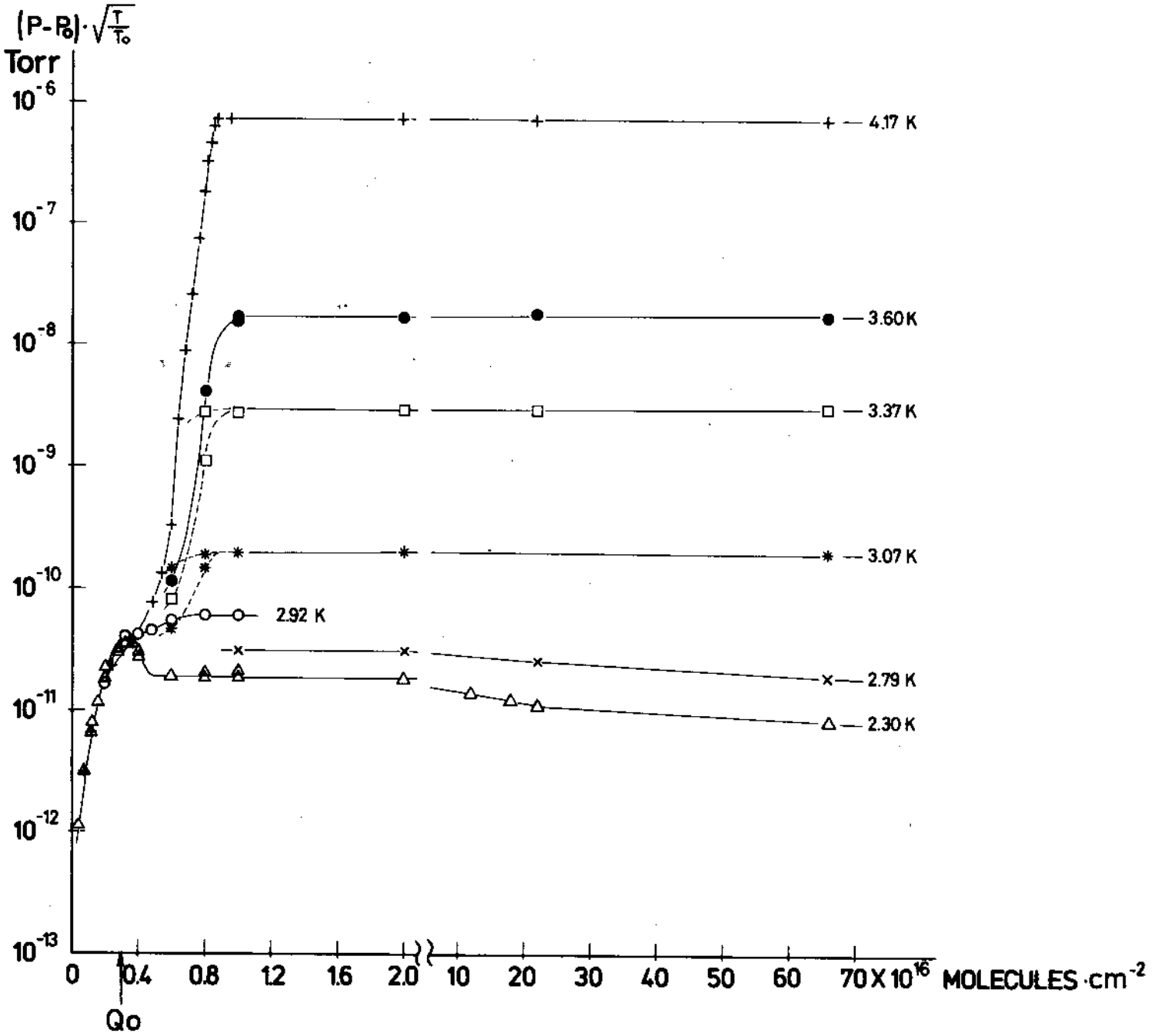

Fig. 7. Adsorption isotherms for H_2, same situation as for Fig. 4.

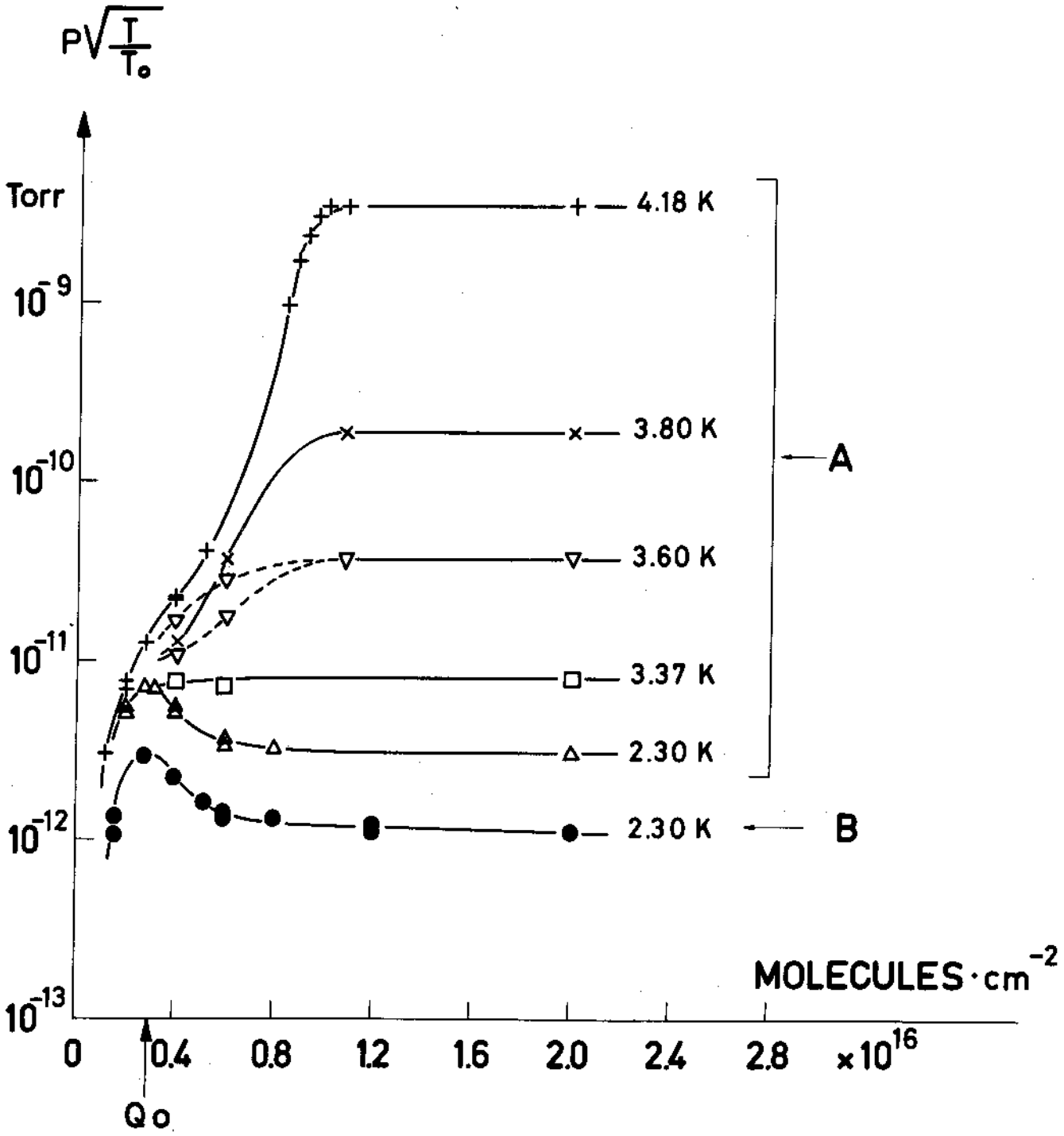

Fig. 8. Adsorption isotherms for HD and D_2, same situation as for Fig. 5. The HD and D_2 contributions from P_o are zero.

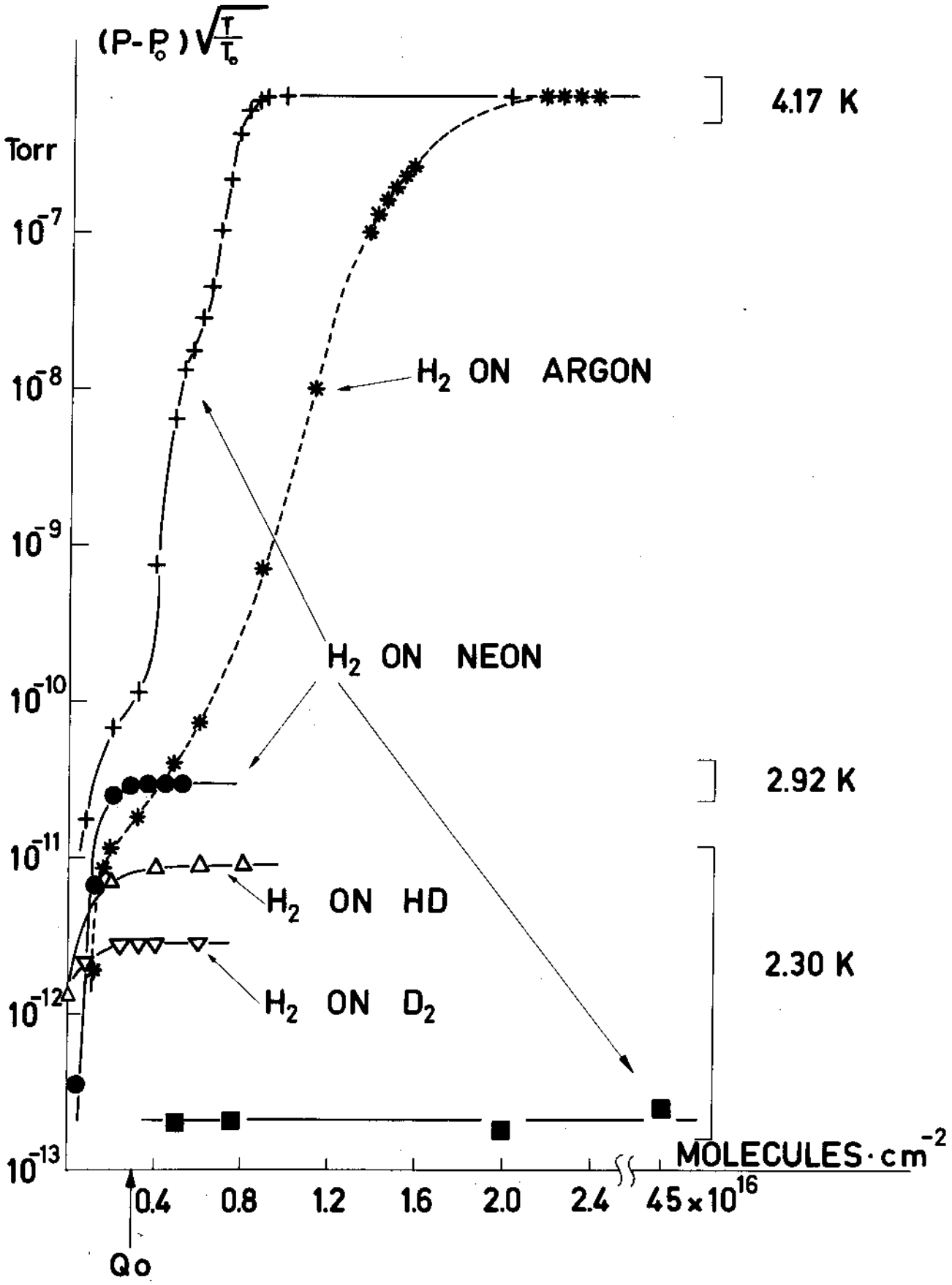

Fig. 9. Adsorption isotherms for H_2 on various precondensed gas layers.
All the measurements have been obtained by means of the model B cryopump, i.e. in the situation described for figures 4 and 7.

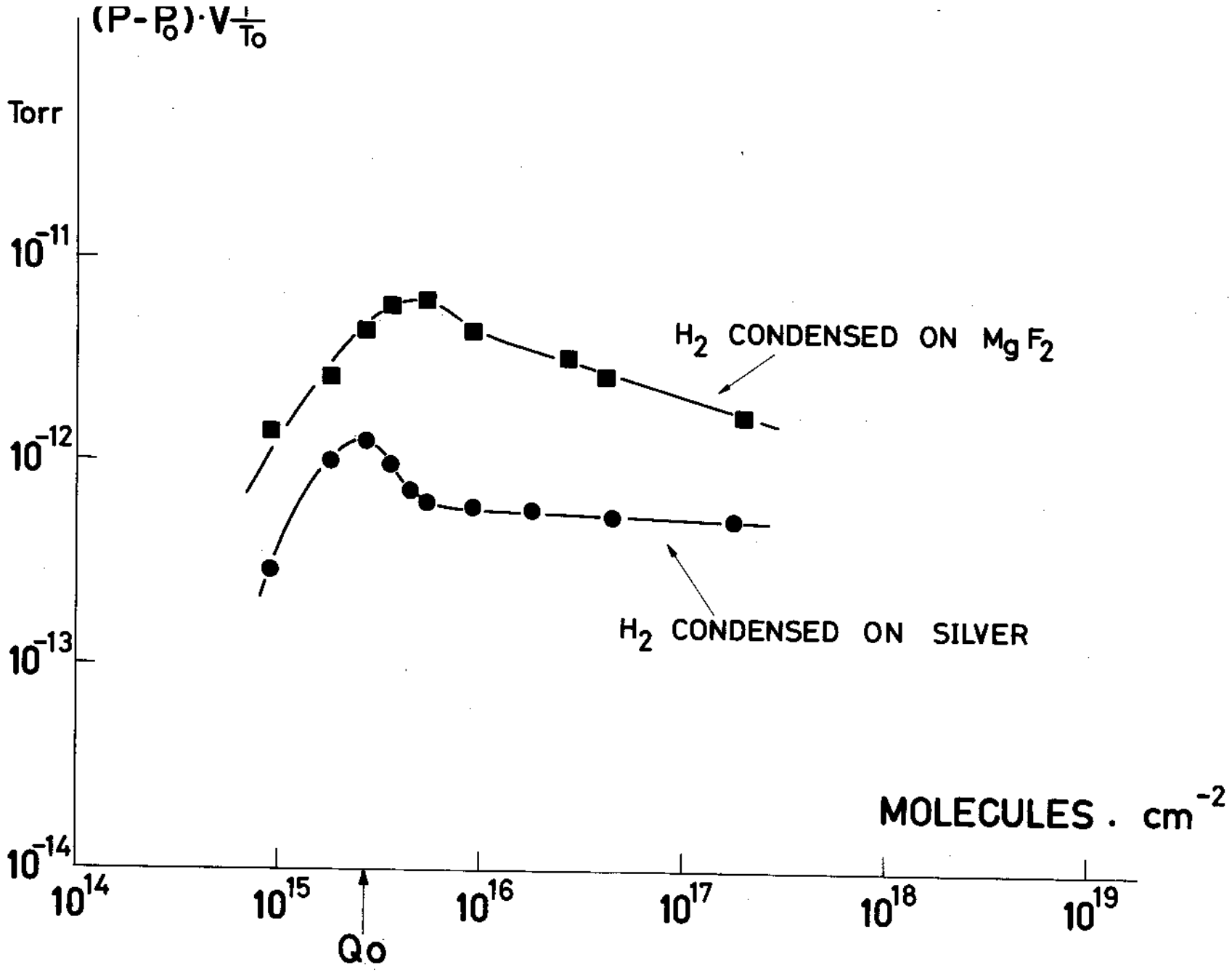

Fig. 10. Adsorption isotherms at 2.3 K for H_2 on MgF_2 (model C cryostat) and on Ag (model E cryopump). In both cases the radiation reaching the cryosurfaces originates at about 80 K (the transmission of the 300 K radiation is below 10^{-4}).

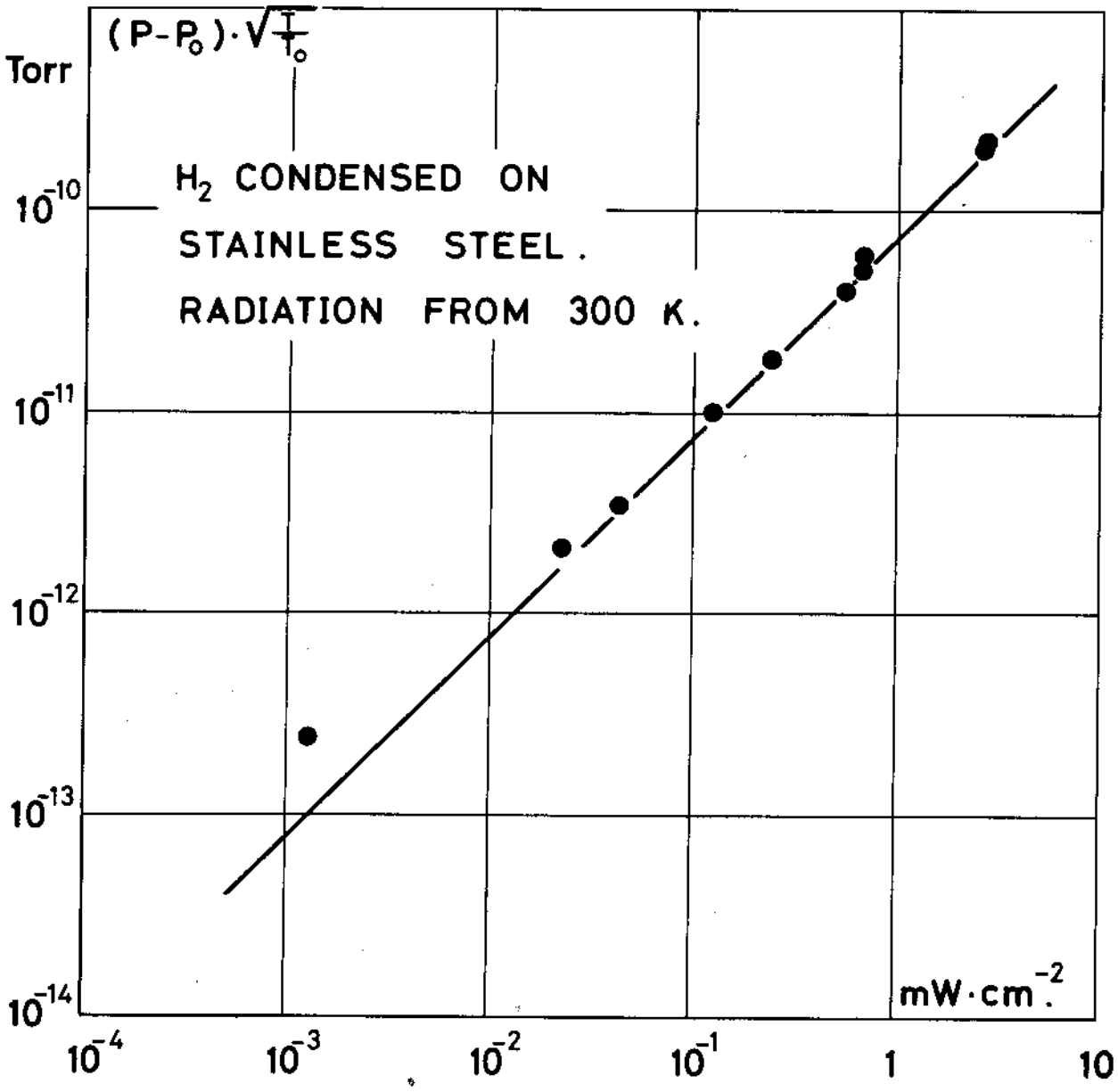

Fig. 11. Dependence of the H_2 saturated vapour pressure at 2.3 K on the thermal radiation power absorbed by the cryosurface.

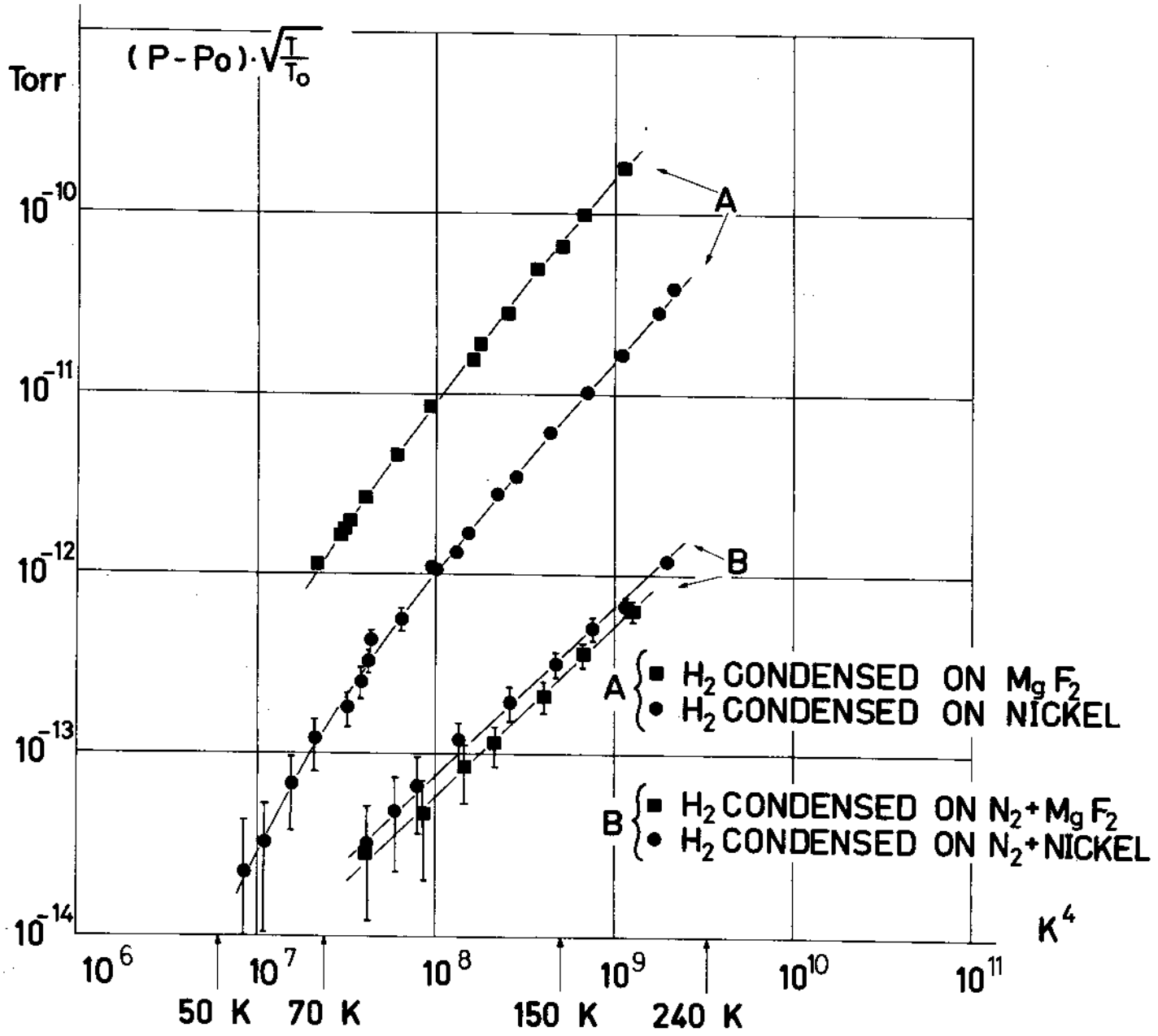

Fig. 12. Radiation-induced H_2 saturated vapour pressure (at 2.3 K) versus the fourth power of the radiating surface temperature for various cryosurfaces. The full lines A and B represent equation (3) (with λ_o = 45 μ) and equation (4), respectively. All measurements have been obtained by raising T.

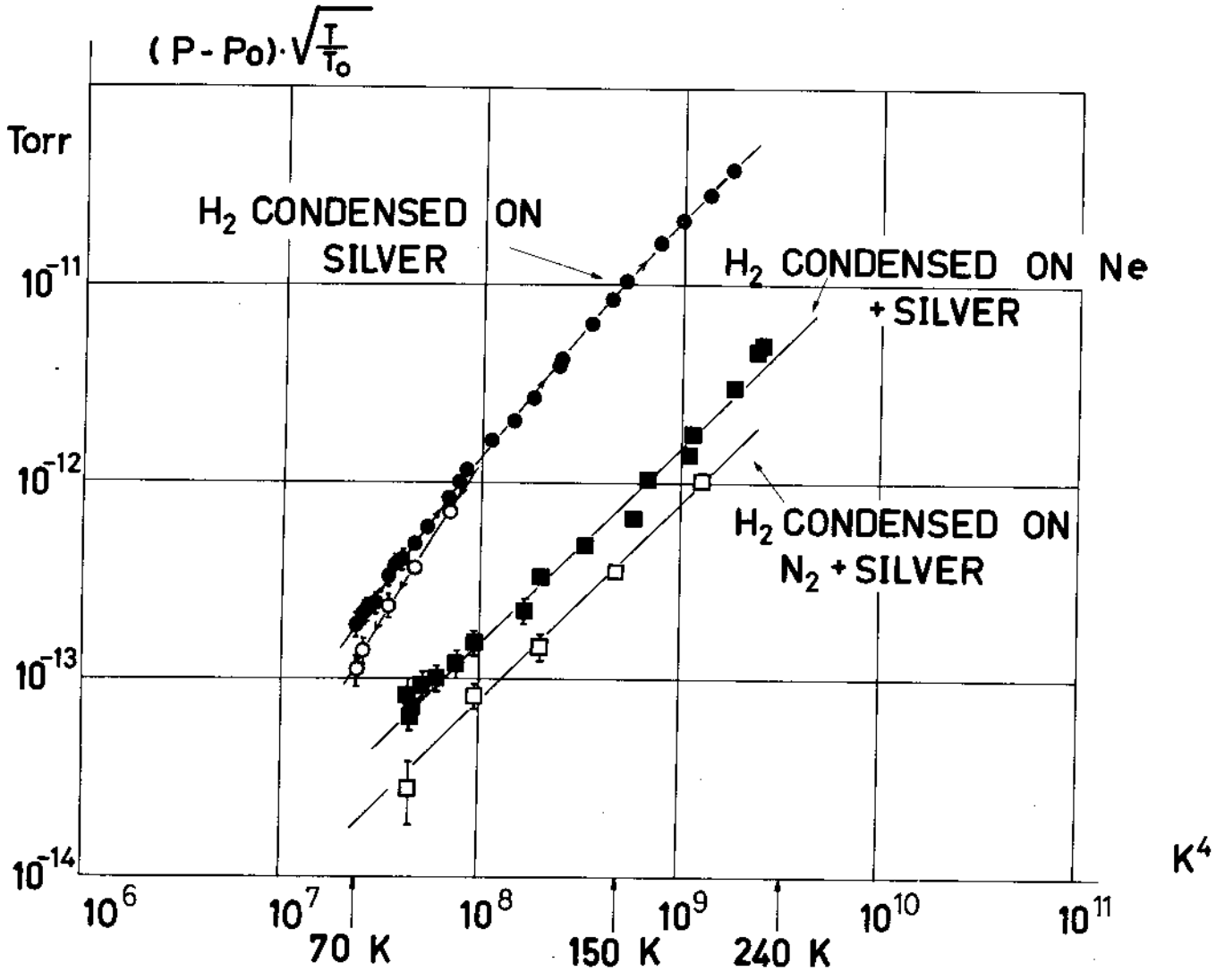

Fig. 13. Same as for Fig. 12. The open circles now represent measurements obtained while lowering T.

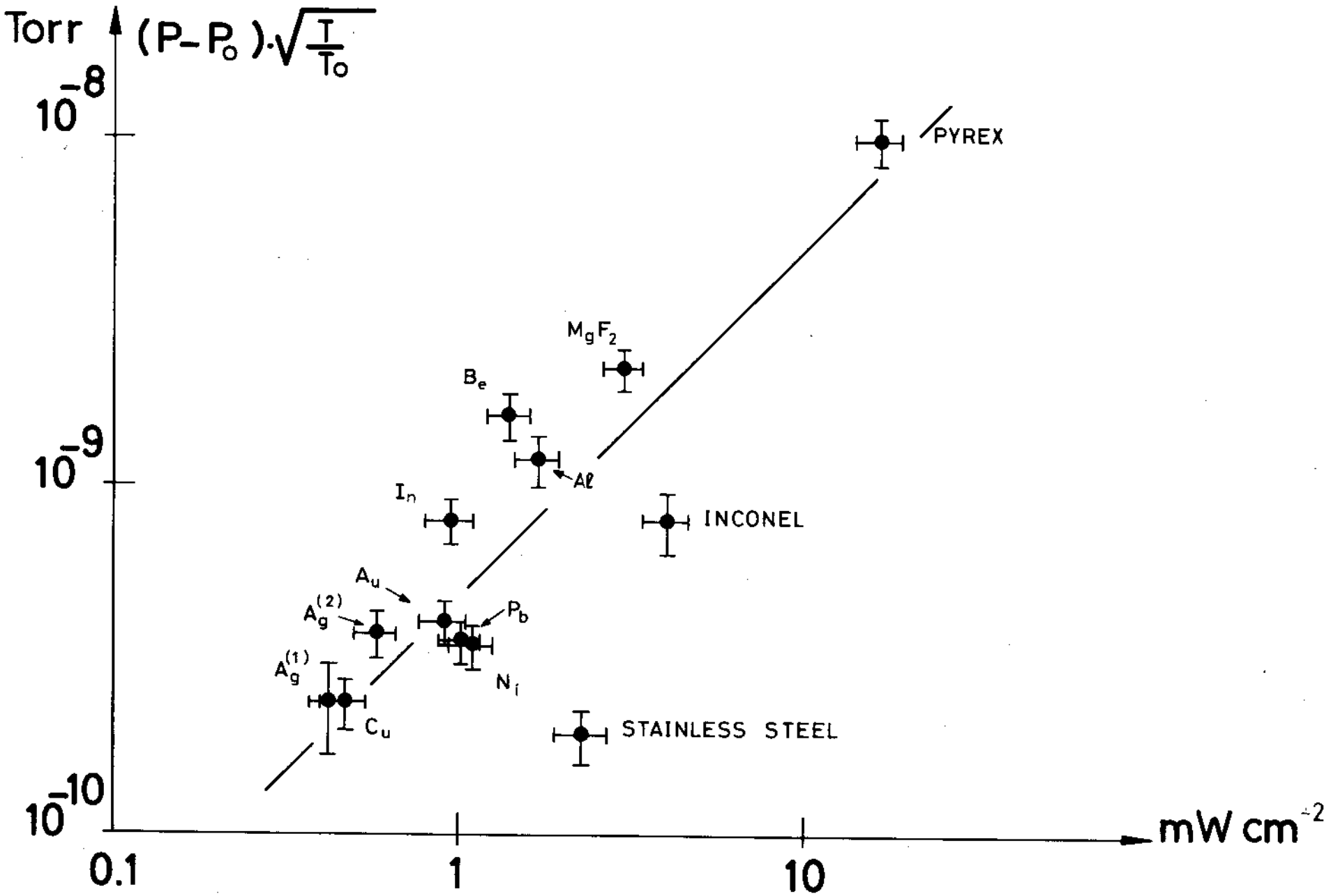

Fig. 14. Saturated vapour pressures of H_2 condensed on different cryosurfaces (at 2.3 K and fully exposed to radiation from 300 K) versus the radiation power absorbed. The line represents the best fit with slope 1 to plotted results.